Chapter 4

Seasonal and Regional Variability of the Complementary Relationship Between Actual and Potential Evaporations in the Asian Monsoon Region

Hanbo Yang and Dawen Yang

Additional information is available at the end of the chapter

http://dx.doi.org/10.5772/53067

1. Introduction

The concept of the complementary relationship (CR) between actual and potential evaporations was first proposed by Bouchet [1]. The underlying argument of the CR can be developed as follows. For one reason independent of energy considerations, actual evaporation LE decrease below wet environment evaporation LE_w, a certain amount of energy not consumed in evaporation becomes sensible heat fluxΔH, which can be expressed as

$$LE_w - LE = \Delta H \tag{1}$$

At the regional scale, this residual energy ΔH affects temperature, humidity, and other variables of air near the ground surface, which lead to an increase in potential evaporation LE_p, and one will have

$$LE_p = LE_w + \Delta H \tag{2}$$

Combination of equations (1) and (2) yields the complementary relationship

$$LE + LE_p = 2LE_w \tag{3}$$

Theoretically, the CR has been heuristically proven based on a series of restrictive assumptions [2, 3]. Also, it has been proved in many applications, such as interpreting the evaporation paradox and estimating actual evaporation. The evaporation paradox was referred as that an increase in actual evaporation estimated by water balance methods over large areas, and a decrease in pan evaporation from measurements in many regions have been recently reported [4, 5], which can be interpreted based on the CR [6]. Using the CR, Brutsaert [7] estimated actual evaporation increase at about 0.44 mm/a2, according to typical values of global trends of net radiation, temperature and pan evaporation. Direct measurement of actual evaporation over large areas is still difficult [8]. Consequently, the CR in which the feedback of potential evaporation with actual evaporation is considered suggests an attractive method for estimating *LE* over a large region, without knowing underlying surface conditions such as soil moisture. This has been widely applied for actual evaporation estimation over different time scales, such as monthly [9-13], daily [14, 15], and hourly [16].

Nevertheless, it was found that the Bouchet hypothesis (Equation 3) was only partially fulfilled [17,18]. In fact, Bouchet [1] documented that Equation (3) was generally modified with consideration of changes to water vapor and energy exchanges of the system with its surroundings, so that $LE + L\ E_p \le 2L\ E_w$. Whereupon the expression was modified [19, 20] as $LE + L\ E_p = mL\ E_w$, where m is a constant of proportionality. Based on 192 data pairs from 25 basins over the United States, Ramirez et al. [19] determined a mean m of 1.97, but with high observed variability.

In the CR, wet environment evaporation (LE_w) was suggested [14] to be given by the Priestley-Taylor equation [21]:

$$LE_w = \alpha \frac{\Delta}{\Delta + \gamma}\left(R_n - G\right) \tag{4}$$

where α is a parameter,.Δ. (kPa/oC) is the slope of saturated vapor pressure at the air temperature, γ (kPa/oC) is a psychometric constant, R_n (mm/day) is net radiation, and G (mm/day) is soil heat flux. Central to wet environment evaporation is the concept of equilibrium evaporation. According to a theory for surface energy exchange in partly open systems, embracing a fully open system and fully closed system as limits, Raupach [22] asserted that a steady state with a steady-state LE_w could be attained; the time to reach steady state (a steady proportion of available energy transforming into latent heat $\alpha \frac{\Delta}{\Delta + \gamma}$) was 1–10 hours for a shallow convective boundary layer. Because of water vapor and energy exchanges between the system and surroundings, the proportion of available energy transforming into latent heat is usually modified. Raupach [23] parameterized the effect of air exchange between system and surroundings on equilibrium evaporation, and suggested conservation equations for entropy and water vapor in an open system. This revealed that advection was likely to modify air temperature and entropy at the system reference height, causing change in the proportion $\alpha \frac{\Delta}{\Delta + \gamma}$.

http://dx.doi.org/10.5772/53067

On calculating LE_w in the CR, Brutsaert and Stricker [14] suggested an average α on the order of 1.26–1.28. The value α=1.32 was predicted by Morton [11]. Hobbins et al. [9] obtained a value of α=1.3177 using data from 92 basins across the conterminous United States. Xu and Singh [24] determined α values in the advection-aridity (AA) model of Brutsaert and Stricker [14] for three study regions at 1.18, 1.04, and 1.00. Yang et al. [25] furnished an average α=1.17 with range 0.87–1.48 from 108 catchments in the Yellow River and Hai River basins of China, whereas Gao et al. [26] suggested an α of 1–1.23 for nine sub-basins of the Hai River basin. Using data from flux measurement stations #40 and #944 from the First International Land Surface Climatology Field Experiment (FIFE) but not in the same period, Pettijohn and Salvucci [27] and Szilagyi [20] obtained different values ofα, 1.10 and 1.18 (or 1.15), respectively. According to data from Weishan flux measurement station, Yang et al. [28] indicated an α range of 1–1.5 for a daytime hourly average. These variable values of the Priestley-Taylor parameter α may imply the variability of the CR.

Under the condition without water limitation, LE equals LE_p, and thus Equation (3) transforms into

$$LE = LE_w \tag{5}$$

This provides a simplified condition to study CR variability. According to analysis of saturated surface evaporation, Priestley and Taylor [21] gave an α range from 1.08 to 1.34, and took 1.26 as the average. Numerous papers report an average α of 1.26 [29-32]. Nevertheless, some details about α in these studies are noteworthy. Means in June, July and September were 1.27, 1.20 and 1.31, respectively [29], and α was less than 1.26 when LE was large, maybe in June or July [31]. Additionally, data in these studies were obtained only in particular months of the year, such as September and October [30], June to September [29], July [31], and June, July and September [32]. Using observations from April to October over a large, shallow lake in the Netherlands, [33] found α had a seasonal variation from 1.20 in August to 1.50 in April. Seasonal variation of α in the Priestley-Taylor equation for calculating LE_w can be considered an indicator of CR variability.

This chapter tried to examine quantitatively the seasonal and regional variability of the CR on the basis of observation data from 6 flux experiment sites and 108 catchments in the Asian monsoon region, and then to find an explanation for CR seasonal and regional variability.

2. Study area and data available

2.1. Flux experiment sites

A flux observation data set was collected from six flux experiment sites (the information was shown in Table 1 and Figure 1). These sites covered a wide range of climate and vegetation conditions from low latitude to high latitude in Asia. Therein five sites belong to the GEWEX (Global Energy and Water cycle Experiment) Asian Monsoon Experiment (GAME), in-

cluding the Kogma site in the Thailand, Tibet_MS3637 site (renamed as Tibet site in this paper) and Hefei site in China, Yakutsk site and Tiksi site in Russia. Another site (Weishan experiment site) was located at the downstream of the Yellow River, China, which was set up by Tsinghua University. This data set includes meteorological elements (air temperature, relative humidity, wind direction and speed, air pressure), radiation (longwave and shortwave radiation, net radiation), soil temperature, precipitation, soil moisture, skin temperature, sensible heat flux, latent heat flux, and soil heat flux. Data were recorded as hourly averages. The energy balance closure problem was solved before data release at five of the six sites except Weishan site. At Weishan site, closure of the energy balance of approximately 0.8 was evaluated, according to data from 2005 to 2006.

The Kogma watershed is covered by a hilly evergreen forest in which only a few species lose their leaves, and canopy top is about 30 m [34, 35]. The Kogma site, part of the GEWEX (Global Energy and Water Cycle Experiment) Asian Monsoon Experiment (GAME), is located in the Kogma watershed of northern Thailand, with a 50 m observation tower. Air temperature and humidity were measured at 43.4 m using a psychrometer (HMP45D, Vaisala). Wind speed was measured at 43.4 m using an anemometer (AC750, Makino Ohyosokki). Downward and upward solar radiations were measured with pyranometers (MS-801 and MS-42, Eiko Seiki Co.) at 50.5 and 43.4 m, respectively. Downward and upward long-wave radiations were measured with an infrared radiometer (MS-200, Eiko Seiki Co.) at 50.5 and 43.4 m. Sensible and latent heat flexes were measured using the eddy correlation system, and the sonic anemometer-thermometer (DA-600, Kaijo) was installed at 41.5 m. Soil heat flux was measured using a probe (MF81, Eiko Seiki Co.)

The Tibet site was setup on May 1998 in the wet grassland between Amdo and Naqu, in the GAME-Tibet region, which was closed in September 1998. Air temperature and humidity were measured using sensors (50Y, Vaisala) at 7.8 and 2.3 m. Wind speed was measured at 9.8 m using an anemometer (R.M. Young Prop-Vane). Downward and upward solar radiations were measured with two pyranometers (CM21, Kipp-Zonen) respectively. Downward and upward long-wave radiations were measured with two pyrgeometers (PSP, Eppley). Sensible and latent heat flexes were measured using the eddy correlation system with a sonic anemometer- thermometer (R3A, Gill). Soil heat flux was measured with a probe (HFT-3.1, REBS).

The Hefei site is set up in the Shouxian Meteorological Observatory, Anhui province for surface flux observation in the Huaihe River Basin. The vegetation of surrounding area consists of mostly rice paddy and partly farmland. Shouxian is located in the middle of intensified observation area of GAME-HUBEX. Air temperature and humidity were measured using sensors (50Y, Vaisala). Wind speed was measured at 9.8 m using an anemometer (09101, R.M. Young Prop-Vane). Downward and upward solar radiations were measured with two pyranometers (Kipp-Zonenn), respectively. Downward and upward long-wave radiations were measured with two pyrgeometers (PIR, Eppley). Sensible and latent heat flexes were measured using the eddy correlation system with a sonic anemometer- thermometer (Gill). Soil heat flux was measured with a probe (HFT-3.1, REBS).

http://dx.doi.org/10.5772/53067

The Yakutsk site is located in the middle reaches of the Lena and is in a region of continuous permafrost, the Sakha Republic of Russian, where the climate exhibits a strong continentality [36]. Air temperature and humidity were measured using sensors (HMP-35D, Vaisala) at 17.2 and 13.4 m. Wind speed was measured at 9.8 m using an anemometer (AC-750, Makino). Downward and upward solar radiations were measured with pyranometers (CM-6F, Kipp-Zonen) at 18.2 and 15.9, respectively. Downward and upward long-wave radiations were measured with pyrgeometers (MS-201F, EKO). Sensible and latent heat flexes were measured using the eddy correlation system with a sonic anemometer- thermometer (DA-600, KAIJO) and an open pathe H2O gas analyser (AH-300, KAIJO).

The Tiksi site is performed in the Siberian tundraregion near Tiksi, Sakha Republic, Russian Federation. Air temperature and humidity were measured using sensors (HMP-45D, Vaisala) at 10 m. Wind speed was measured at 10 m using an anemometer (AC860, Makino). Downward solar radiation was measured at 1.5 m with a pyranometer (MS-802F, EKO). Downward and upward long-wave radiations were measured at 1.5 m with pyrgeometers (MS-802F, EKO). Sensible and latent heat flexes were measured using the eddy correlation system with a sonic anemometer- thermometer. Soil heat flux was measured with a probe (MF-81, EKO) at 0.01 and 0.08 m. More details about the five sites are provided at the GAME website (http://aan.suiri.tsukuba.ac.jp/).

Site	**Location**	Altitude (m)	Vegetation type	**Data period**
Kogma	18°48.8'N, 98°54.0'E	1268	Evergreen forest	Feb. – Dec., 1998
Tibet	31°01.0'N, 91°39.4'E	4820	Grass	May – Sep., 1998
Hefei	32°34.8'N, 116°46.2'E	23	Rice paddy	Aug., 1998 , Apr., Nov., and Dec., 1999
Weishan	36°38.9'N, 116°03.3'E	30	Wheat, corn	May 18, 2005 – Dec. 31, 2006
Yakutsk	62°15.3'N, 129°37.1'E	210	Larch forest	Apr. – Aug., 1998 Apr. – Jul., 1999
Tiksi	71°35.2'N, 128°46.5'E	40	Tundra	Jun. – Sep., 2000

Table 1. Descriptions of the flux experiment sites

The Weishan site is located in a downstream reach of the Yellow River. Most of this region is farmland, with flat topography. Winter wheat and maize are the two major crops, rotationally cultivated [37]. Winter wheat planting season is in early October, and the growing period is from March to mid-June. The experimental field is near the center of the irrigation district, and is a 400 m by 500 m rectangular field. Typical meteorological instruments are installed atop a 10 m tall tower, along with a radiometer and an eddy correlation system for sensible and latent heat fluxes. Air temperature and humidity were measured using sensors (HMP-45C, Vaisala) at 10 m. Wind speed was measured at 10 m using an anemometer (05103, Young Co.). Downward and upward solar and long-wave radiations were measured

at 3.5 m with pyranometers (CNR-1, Kipp-Zonen). Sensible and latent heat flexes were measured using the eddy correlation system at 3.7 m with a sonic anemometer-thermometer (CSAT3, Campbell). Soil heat flux was measured with a probe (HFP01SC, Hukseflux). Observations were recorded as 30-minute averages.

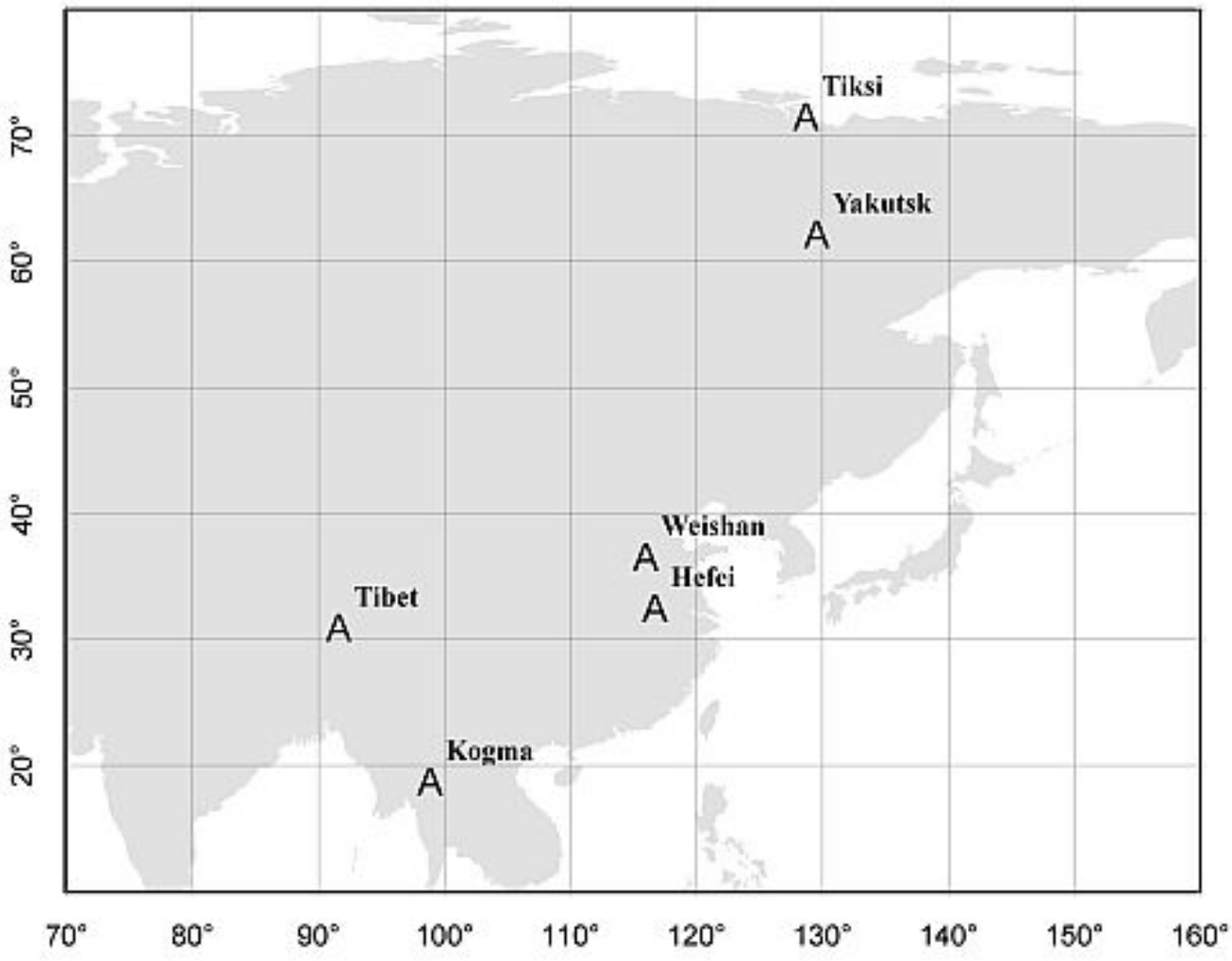

Figure 1. Location of the two flux experiment sites

2.2. Study catchments

To examine the regional variability, 108 catchments, locating in the Yellow River basin, the Hai River basin, and the Inland Rivers basin in the non-humid region of China were chose. Their drainage areas cover a range 272–94,800 km^2. Climate arid index covers from 1–7, and the runoff coefficient ranges 0.02–0.32. The hydrologic and meteorological data were collected from each catchment from 1953–1998. Figure 2 presents the distribution of hydrologic and meteorological stations in the study region. Furthermore, more information on the 108 catchments was given by [38].

http://dx.doi.org/10.5772/53067

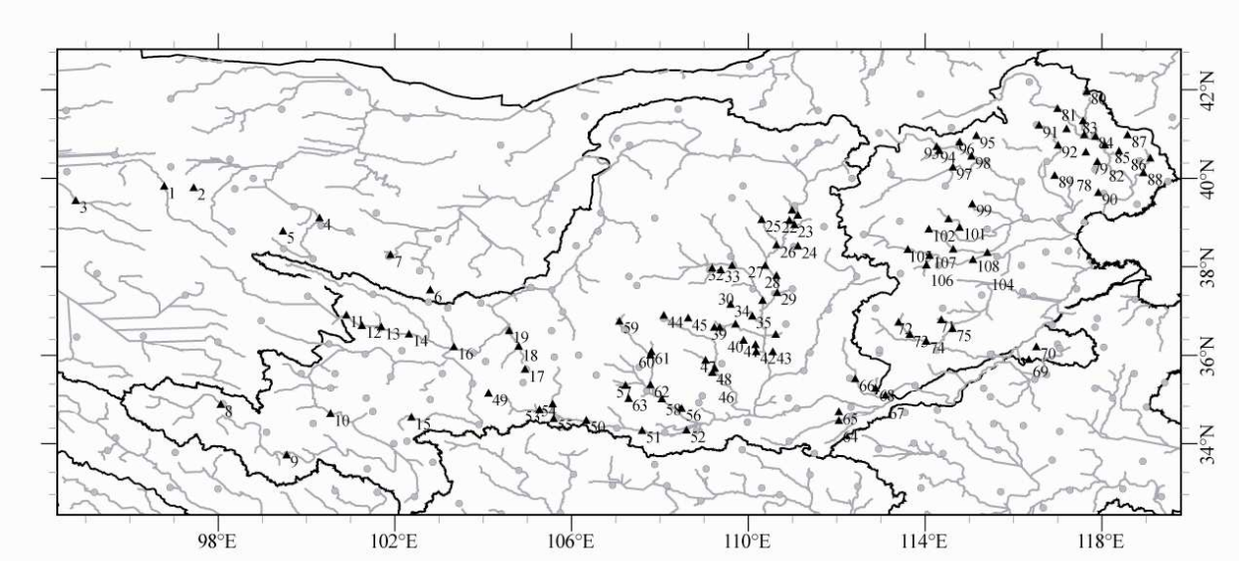

Figure 2. Distribution of the hydrologic and meteorological stations in the 108 catchments in the non-humid regions of China (the solid triangle represents a hydrologic station at the outlet of catchments and the grey solid circle represents a meteorological station)

3. Method

In a closed system without advection, the CR can be expressed as equation (3) in which LE_w is estimated using equation (4) with $\alpha = 1.26$. However, in a real open environment the horizontal advection can't be neglected. Therefore, taking the effect of the horizontal advection into account, we have two methods, and the one is

$$A = LE + LE_p - 2 \times 1.26 \frac{\Delta}{\Delta + \gamma}\left(R_n - G\right), \tag{6}$$

i.e., the CR is modified as$LE + L\ E_p = 2L\ E_w + A$. The value of A indicated the effect of the horizontal advection of both energy and water vapor. Morton [10] suggested a similar equation$LE + L\ E_p = 2 \times 1.26 \frac{\Delta}{\Delta + \gamma}(R_n - G + A_m)$, where A_m was an empirical correction factor for advection. If there is a seasonal and regional variability in the CR, Ashould have a seasonal and regional variation. The other one is focusing on the Priestley-Taylor parameter α to reveal seasonal and regional variability of the CR. According to Equations (3) and (4), αcan be calculated as

$$\alpha = \frac{\gamma + \Delta}{2\Delta} \cdot \frac{LE + LE_{\mathrm{p}}}{R_{\mathrm{n}} - G} \tag{7}$$

Similar to A, α should have a seasonal and regional variation if there is a seasonal and regional variability in the CR.

The wet environment evaporation LE_{w} was estimated by the Priestley-Taylor equation. To calculate potential evaporation LE_{p}, the Penman equation [39] has been suggested by [10, 14, 40]

$$LE_{\mathrm{p}} = \frac{\Delta}{\Delta + \gamma}\left(R_{\mathrm{n}} - G\right) + \frac{\gamma}{\Delta + \gamma} E_{\mathrm{A}}, \tag{8}$$

where E_{A} is the drying power of the air. This can be estimated by

$$E_{\mathrm{A}} = f(u)\left(e^{*} - e\right), \tag{9}$$

where e^{*} (kPa) and e (kPa) are the saturated and actual vapor pressures at the same air temperature, respectively. The wind function $f(u)$ can be estimated as

$$f(u) = 0.26\left(1 + 0.54u\right), \tag{10}$$

where u (m/s) is mean wind speed at 2 m height.

Actual evaporation LE was observed using the eddy correlation technique at the flux experiment sites, and was calculated from the annual water balance by ignoring the inter-annual change of water storage in these catchments.

4. Results

4.1. Seasonal and regional variability observed in the flux experiment sites

The horizontal advection term A in the modified CR and the Priestley-Taylor parameter α at the six sites were calculated using equations (6) and (7) respectively based on the daily data. Then the daily values were averaged on each ten-day from the starting date, and the results were shown in Figures 3 and 4. With regard to the value of A, Figure 3 shows different variance ranges at different sites. However, a seasonal variation is observable, i.e. the value of A reaches the minimum in July or August, then rises up to the maximum in March or April,

http://dx.doi.org/10.5772/53067

and decreases at last until July or August. Similarly, Figure 4 shows the Priestley-Taylor's parameter α has a seasonal variation with a maximum in winter and a minimum in summer. In general, we discern seasonal variation ofα, although the points are scattered in winter.

In particular, at Kogma, αhas a maximum of 1.7 approximately in February, then falls to a minimum of 1.1 approximately in summer; it increases thereafter, until winter, which ranges from 1.08–1.40 between April and October. At Weishan, αhas a mean of 1.18 during the summer monsoon period, and about 1.92 during the winter monsoon. Monthly α varies from 1.02–1.40 between May and October.

Figure 3 also shows that the Priestley-Taylor's parameter α increases with latitude increasing, which is the largest at the Yakutsk site in Siberia of Russia and the smallest at the Kogma site in Thailand in the same season.

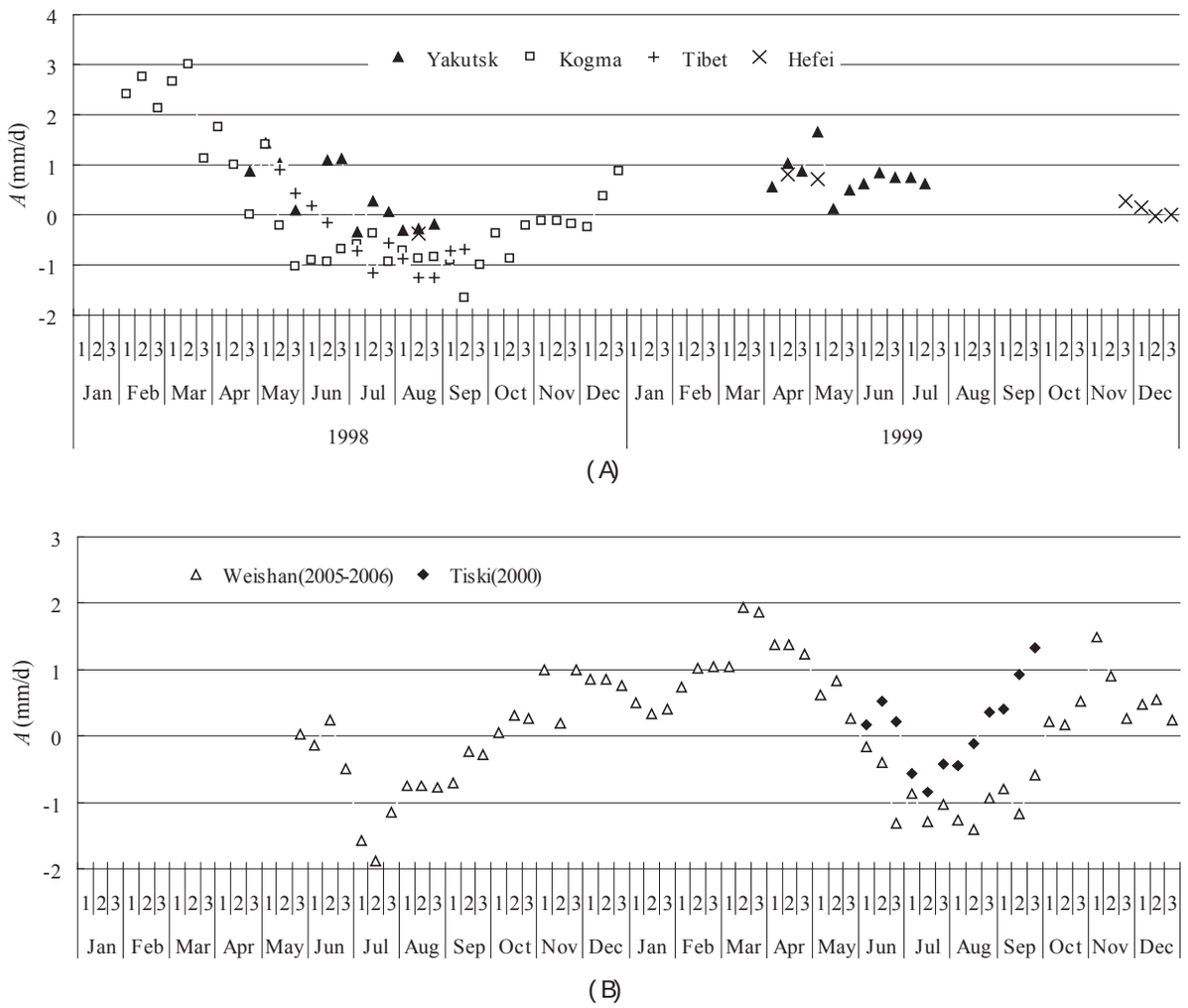

Figure 3. Seasonal and regional variability of the horizontal advection.

4.2. Regional variability observed in the 108 catchments

The parameter α for the 108 catchments has a large variance, which ranges from 0.87 to 1.48 (with an average of 1.17). Nevertheless, the relation of α with latitude can be revealed, as shown in Figure 3. The parameter α increases with the latitude increasing over the region ranging 33–40 °N, while it decreases with the latitude increasing over the region ranging 40–42 °N. Also, the relation of the parameter α with the longitude was plotted in Figure 4. It can be found that the catchment with larger longitude is approximately closer to the ocean. Therefore, Figure 4 shows that α increases with the distance from ocean decreasing.

5. Discussion

5.1. Seasonal variability

The value of A reaches the minimum in July or August, then rises up to the maximum in March or April, and decreases at last until July or August. As shown in Figure 4, the Priestley-Taylor's parameter α has a seasonal variation with a maximum in winter and a minimum in summer [41], which is similar to that A has. Also, most studies did not introduce an advection item, but instead adjusted the Priestley-Taylor parameter for advection. Therefore, we focus on the variation of α in this chapter.

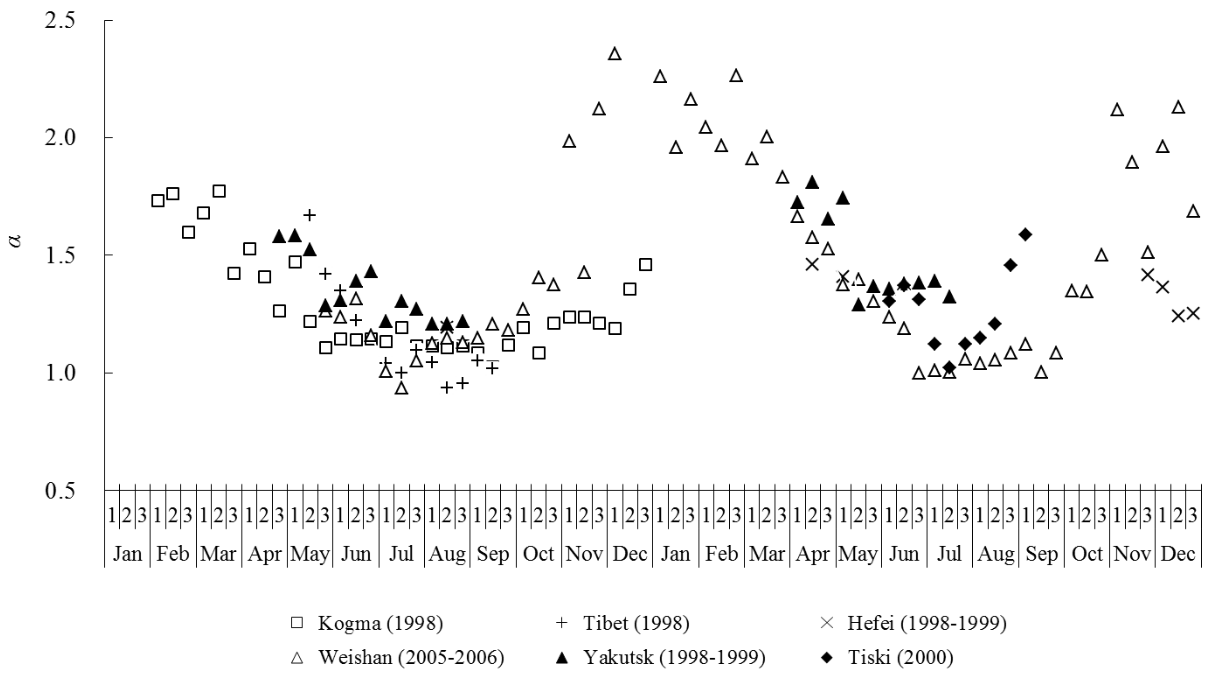

Figure 4. Seasonal and regional variability of the Priestley-Taylor's parameter α

http://dx.doi.org/10.5772/53067

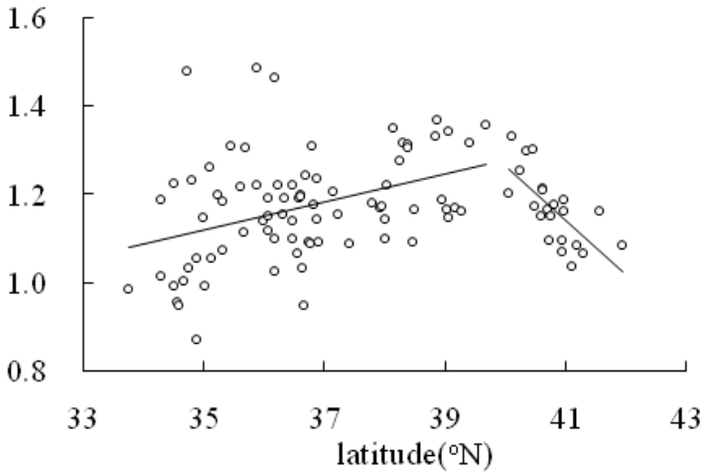

Figure 5. Relation of parameter α with latitude

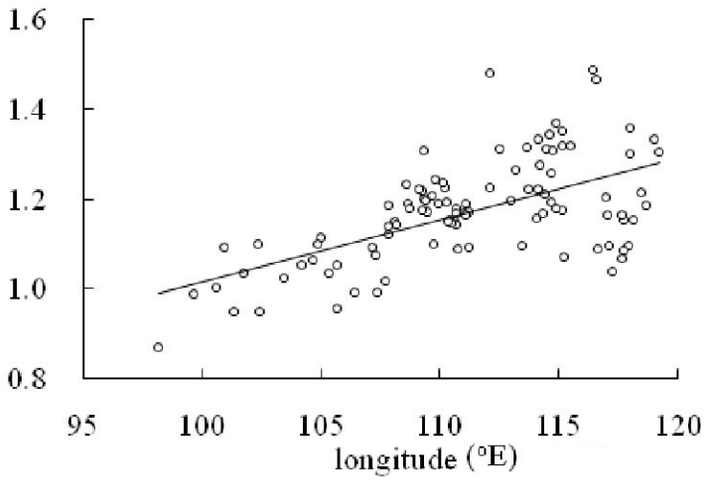

Figure 6. Relation of parameter α with longitude (larger longitude indicating the catchment being nearer the ocean)

DeBruin and Keijman [33] reported that α differed slightly from 1.26 in May–September, but was about 1.50 in April and October. Similarly, the α value at Kogma was between 1.07–1.26 in May–September and was 1.40 in April. At the Weishan site, αhad a similar seasonal variation but larger values, up to 1.60 in April and 1.38 in October. At the same time, another phenomenon, that the Asian monsoon is from ocean to continent in June–October and from continent to ocean in October–June [42], should be noticing. As a result, the monsoon leads to air temperature decreasing and humid increasing in June–October, while both air temperature and humidity increasing in October–June above the continent. It was therefore speculated that there is a certain relation between the seasonal variation in α and the monsoon.

The energy balance near the ground surface can be expressed as

$$R_n - G = LE + H \tag{11}$$

Advection impacts the CR by modifying air temperature, water vapor pressure, and others. As a result, the partition of available energy into latent and sensible heats will change, and the presence of advection causes $LE > R_n - G$ [43-45] when the direction of sensible heat H is downward. Differences in thermodynamic properties between land and ocean produce generally higher temperatures and less water vapor over continents than over oceans in summer, and lower temperatures and less water vapor over continents than oceans in winter. Consequently over continents, atmospheric circulation between land and ocean decreases temperature and increases vapor during summer, and increases both temperature and vapor in winter. It seems paradoxical that the winter monsoon increases temperature over continents. In fact, we find that the distribution of isotherms is not completely latitudinal; temperature has an inverse relationship with distance from the ocean in identical latitude continental regions. This indicates heat transport from ocean to continent by advection. We speculate that the circulation increases temperature over land, and the increase weakens with distance from the ocean, as a result of sensible heat transport.

Advection possibly affects the major assumption of the CR, that energy release from a decrease in actual evaporation compensates the increase in potential evaporation [46]. The monsoon transports water vapor and sensible heat between ocean and continent, which causes additional seasonal changes to air humidity and temperature. The effects of these changes on the two sides of Equation (3) are asymmetric. On the left side, the terms LE_p and LE can be determined by climate variables (such as air temperature and vapor pressure), which include the effect of horizontal advection. On the right side, the effect of horizontal advection on LE_w is parameterized as only the change of air temperature (if the effect of radiation is neglected), not including changes of wind speed and humidity.

We assume a system without horizontal advection, where Equation (3) is satisfied. Since the summer monsoon imports a large amount of water vapor and reduces latent heat, the drying power of the air E_A decreases, and increases the ratio $H/(R_n - G)$ (i.e., LE decreases). This reduces $(LE + LE_p)$ but causes less change in LE_w. This translates into a smaller α in Equation (3). The winter monsoon increases E_A and $LE/(R_n - G)$, which produces an increase in $(LE + LE_p)$ but less change in LE_w, resulting in a larger in Equation (3). Following the same reasoning, we can explain the seasonal variation in α revealed by [33]. According to the CR, with an unlimited water supply above a lake, the evaporation LE equals the potential evaporation LE_p. In summer, horizontal advection reduces $(LE + LE_p)$, resulting in a small α value, but a large α in winter.

5.2. Regional variability

In addition, the effect of horizontal advection also has a regional variation. Since energy is transported by atmospheric and oceanic circulations from low to high latitudes, and water

http://dx.doi.org/10.5772/53067

vapor transported from the lower atmospheric layer over the ocean to that over land. This therefore leads to a regional variability in the CR.

From the Figure 3, it can be seen that the magnitude of the horizontal advection effect is the largest at the Yakutsk site and the smallest at the Kogma site in the same season. This indicates that the magnitude of the horizontal advection effect increases with latitude increasing. Figure 4 shows that the Priestley-Taylor's parameter α increases with latitude increasing, which is the largest at the Yakutsk site and the smallest at the Kogma site in the same season. This is also consistent with the results given by Xu and Singh [23], in which α =1.0, 1.04 and 1.18 at the catchments in Eastern China (29°15′N, 121°10′E), Northwestern Cyprus (about 35°N), and Central Sweden (59°53′N, 17°35′E) respectively for a long-term mean.

Across the 108 catchments, the parameter α increases with the latitude increasing over the region ranging 33–40 °N but decreases with the latitude increasing over the region ranging 40–42 °N. As shown in Figure 2, the catchments ranging 40–42 °N belong to the Hai River basin, which are adjacent to the Bohai Sea. Those catchments have an increasing distance from the sea with their latitude increasing. The possible cause is that the change in distance from the sea has a larger effect on the horizontal advection than increasing latitude has. This was revealed by Figure 6, i.e. the catchments farther from the sea have larger parameterα. In addition, Figure 6 shows larger dispersion in the relation between α and the longitude, the possible cause for which was that the flexuous coastline results in the catchments with same longitude having different distance from the ocean.

6. Conclusion

The complementary relationship (CR) between actual evaporation and potential evaporation has been widely used to explain the evaporation paradox, as well as to estimate regional evaporation. The theoretical foundation of the CR is the Bouchet hypothesis, including the constraint that exchanges of water vapor and energy between the considered system and its exterior are constant. In reality, the atmosphere does not always satisfy the constraint. In the Asian monsoon region, atmospheric motions have a significant seasonal variation, accompanied by transport of water vapor and energy. Through analyzing seasonal variation in parameter α of the Priestley-Taylor equation for calculating wet environment evaporation, this chapter analyzed effects of horizontal advection on the CR. αhas a significant seasonal variation, which is larger in winter than in summer. The possible cause is that the summer monsoon increases water vapor content and decreases air temperature, whereas the winter monsoon increases both water vapor and air temperature. The parameter α increases with latitude, as a result of the annual transport of the energy and vapor from low latitudes to high latitudes through the atmospheric and oceanic flows. Atmospheric circulation between continent and ocean transports vapor from the oceans to the land, so α decreases with distance from ocean.

Acknowledgements

Data were from the Global Energy and Water Cycle Experiment (GEWEX) Asian Monsoon Experiment in a Tropical region (GAME-T), and Weishan flux observation was supported by the National Natural Science Foundation of China (grant nos. 50909051, 50939004, and 51025931). This research was also supported by the Ministry of Science and Technology of China (2011IM011000).

Author details

Hanbo Yang* and Dawen Yang

*Address all correspondence to: yanghanbo@tsinghua.edu.cn

State Key Laboratory of Hydro-Science and Engineering, Department of Hydraulic Engineering, Tsinghua University, Beijing, China

References

[1] Bouchet, R. (1963), Evapotranspiration reelle evapotranspiration potentielle, signification climatique, Int Assoc Sci Hydrol Proc, 62, 134-142.

[2] Morton, F. I. (1971), Catchment evaporation and potential evaporation: further development of a climatologic relationship, J Hydrol, 12, 81-99.

[3] Szilagyi, J. (2001), On Bouchet's complementary hypothesis, J Hydrol, 246(1-4), 155-158.

[4] Milly, P. C., and K. A. Dunne (2001), Trends in evaporation and surface cooling in the Mississippi River basin, Geophys Res Lett, 28(7), 1219-1222.

[5] Walter, M. T., D. S. Wilks, J. Y. Parlange, and R. L. Schneider (2004), Increasing evapotranspiration from the conterminous United States, J Hydrometeorol, 5(3), 405-408.

[6] Brutsaert, W., and M. B. Parlange (1998), Hydrologic cycle explains the evaporation paradox, Nature, 396(6706), 30.

[7] Brutsaert, W. (2006), Indications of increasing land surface evaporation during the second half of the 20th century, Geophys Res Lett, 33, L20403, doi: 10.1029/2006GL027532.

[8] Kahler, D. M., and W. Brutsaert (2006), Complementary relationship between daily evaporation in the environment and pan evaporation, Water Resour Res, 42(5), doi: 10.1029/2005WR004541.

[9] Hobbins, M. T., J. A. Ramirez, and T. C. Brown (2001), The complementary relationship in estimation of regional evapotranspiration: An enhanced Advection-Aridity model, Water Resour Res, 37(5), 1389-1403.

[10] Morton, F. I. (1975), Estimating evaporation and transpiration from climatological observations, Journal of Applied Moteorology, 14, 488-497.

[11] Morton, F. I. (1983), Operational estimates of areal evapotranspiration and their significance to the science and practice of hydrology, J Hydrol, 66, 1-76.

[12] Szilagyi, J., and J. Jozsa (2008), New findings about the complementary relationship-based evaporation estimation methods, J Hydrol, 354(1-4), 171-186.

[13] Szilagyi, J., M. T. Hobbins, and J. Jozsa (2009), Modified Advection-Aridity Model of Evapotranspiration, JOURNAL OF HYDROLOGIC ENGINEERING, 14(6), 569-574.

[14] Brutsaert, W., and H. Stricker (1979), An advection-aridity approach to estimate actual regional evapotranspiration, Water Resour Res, 15(2), 443-450.

[15] Han, S. J., H. P. Hu, D. W. Yang, and F. Q. Tian (2011), A complementary relationship evaporation model referring to the Granger model and the advection-aridity model, Hydrol Process, 25(13), 2094-2101.

[16] Parlange, M. B., and G. G. Katul (1992), An advection-aridity evaporation model, Water Resour Res, 28, 127-132.

[17] Kim, C. P., and D. Entekhabi (1998), Feedbacks in the land-surface and mixed-layer energy budgets, Bound-Lay Meteorol, 88(1), 1-21.

[18] Sugita, M., J. Usui, I. Tamagawa, and I. Kaihotsu (2001), Complementary relationship with a convective boundary layer model to estimate regional evaporation, Water Resour Res, 37(2), 353-365.

[19] Ramirez, J. A., M. T. Hobbins, and T. C. Brown (2005), Observational evidence of the complementary relationship in regional evaporation lends strong support for Bouchet's hypothesis, Geophys Res Lett, 32, L15401, doi:10.1029/2005GL023549.

[20] Szilagyi, J. (2007), On the inherent asymmetric nature of the complementary relationship of evaporation, Geophys Res Lett, 34, L02405, doi:10.1029/2006GL028708.

[21] Priestley, C. H. B., and R. J. Taylor (1972), On the assessment of surface heat flux and evaporation using large-scale parameters, Mon Weather Rev, 100(2), 81-92.

[22] Raupach, M. R. (2000), Equilibrium evaporation and the convective boundary layer, Bound-Lay Meteorol, 96(1-2), 107-141.

[23] Raupach, M. R. (2001), Combination theory and equilibrium evaporation, Q J Roy Meteor Soc, 127(574), 1149-1181.

[24] Xu, C. Y., and V. P. Singh (2005), Evaluation of three complementary relationship evapotranspiration models by water balance approach to estimate actual regional evapotranspiration in different climatic regions, J Hydrol, 308(1-4), 105-121.

[25] Yang, H.B., Yang, D.W., Lei, Z.D., Sun, F.B. and Cong, Z.T., 2008. Reginal varibility of the complementary relationship between actual and potential evapotranspirations (in Chinese). Journal of Tsinghua University (Science and Technique), 48(9): 1413-1416.

[26] Gao, G., C. Xu, D. Chen, and V. P. Singh (2012), Spatial and temporal characteristics of actual evapotranspiration over Haihe River basin in China, Stoch Env Res Risk A, 26(5): 655-669.

[27] Pettijohn, J. C., and G. D. Salvucci (2006), Impact of an unstressed canopy conductance on the Bouchet-Morton complementary relationship, Water Resour Res, 42(9), W09418, doi:10.1029/2005WR004385.

[28] Yang, H. B., D. W. Yang, Z. D. Lei, F. B. Sun, and Z. T. Cong (2009), Variability of complementary relationship and its mechanism on different time scales F-5023-2011 G-4441-2010, Sci China Ser E, 52(4), 1059-1067.

[29] Davies, J. A., and C. D. Allen (1973), Equilibrium, potential, and actual evaporation from cropped surfaces in southern Ontario, J Appl Meteorol, 12, 649-657.

[30] Eichinger, W. E., M. B. Parlange, and H. Stricker (1996), On the concept of equilibrium evaporation and the value of the Priestley-Taylor coefficient, Water Resour Res, 32(1), 161-164.

[31] Stewart, R. B., and W. R. Rouse (1976), A simple method for determining the evaporation from shallow lakes and ponds, Water Resour Res, 12, 623-628.

[32] Stewart, R. B., and W. R. Rouse (1977), Substantiation of the Priestley-Taylor parameter α= 1.26 for potential evaporation in high latitudes, J Appl Meteorol, 16, 649-650.

[33] DeBruin, H. A. R., and J. Q. Keijman (1979), The Priestley-Taylor evaporation model applied to a large shallow lake in the Netherland, J Appl Meteorol, 18, 898-903.

[34] Komatsu, H., N. Yoshida, H. Takizawa, I. Kosaka, C. Tantasirin, and M. Suzuki (2003), Seasonal trend in the occurrence of nocturnal drainage flow on a forested slope under a tropical monsoon climate, Bound-Lay Meteorol, 106(3), 573-592.

[35] Kume, T., H. Takizawa, N. Yoshifuji, K. Tanaka, C. Tantasirin, N. Tanaka, and M. Suzuki (2007), Impact of soil drought on sap flow and water status of evergreen trees in a tropical monsoon forest in northern Thailand, Forest Ecol Manag, 238(1-3), 220-230.

[36] Dolman, A. J., T. C. Maximov, E. J. Moors, A. P. Maximov, J. A. Elbers, A. V. Kononov, M. J. Waterloo, and M. K. van der Molen (2004), Net ecosystem exchange of carbon dioxide and water of far eastern Siberian Larch (Larix cajanderii) on permafrost, BIOGEOSCIENCES, 1(2), 133-146.

[37] Lei, H. M., and D. W. Yang (2010), Interannual and seasonal variability in evapotranspiration and energy partitioning over an irrigated cropland in the North China Plain, Agr Forest Meteorol, 150(4), 581-589.

[38] Yang, D. W., F. B. Sun, Z. Y. Liu, Z. T. Cong, G. H. Ni, and Z. D. Lei (2007), Analyzing spatial and temporal variability of annual water-energy balance in nonhumid regions of China using the Budyko hypothesis, Water Resour Res, 43, W04426, doi: 10.1029/2006WR005224.

[39] Penman, H. L. (1948), Natural evaporation from open water, bare soil and grass, Proceeding of the Royal Society of London. Series A, Mathematical and Physical Sciences, 193(1032), 120-145.

[40] Morton, F. I. (1976), Climatological estimates of evapotranspiration, J. Hydraul. Div. Proc. ASCE, 102, 275-291.

[41] Yang, H. B., D. W. Yang, and Z. D. Lei (2012), Seasonal variability of the complementary relationship in the Asian monsoon region, Hydrol Process, DOI: 10.1002/hyp. 9400.

[42] Ye, D. Z., Tao, S. Y., and Li, M. C., 1958. The abrupt change of circulafion over the Northern Hemisphere during June and October (in Chinese). Acta Meteorologica Sinica, 29, 249-263.

[43] Rijks, D. A. (1971), Water Use by Irrigated Cotton in Sudan. III. Bowen Ratios and Advective Energy, The Journal of Applied Ecology, 8, 643-663.

[44] Rosenberg, N. J., and S. B. Verma (1976), Extreme Evapotranspiration by Irrigated Alfalfa: A Consequence of the 1976 Midwestern Drought, J Appl Meteorol, 17, 934-941.

[45] Wright, J. L., and M. E. Jensen (1972), Peak water requirements of crops in southern Idaho, Journal of Irrigation and Drainage Division, 96, 193-201.

[46] Lhomme, J. P., and L. Guilioni (2006), Comments on some articles about the complementary relationship, J Hydrol, 323(1-4), 1-3.

IntechOpen